Structure of the Ne-Xe mixture near the 26-MPa demixing curve at $T=275$ K

M. Nardone and F. P. Ricci
Dipartimento di Fisica, Università degli Studi di Roma Tre, Unita' di ricerca dell'Istituto Nazionale di Fisica della Materia, Via della Vasca Navale 84, 00146 Roma, Italy

A. Filabozzi
Dipartimento di Fisica, Università di Roma Tor Vergata, Unita' di ricerca dell'Istituto Nazionale di Fisica della Materia, Via della Ricerca Scientifica 1, 00137 Roma, Italy

P. Postorino
Dipartimento di Fisica, Università di Roma ''La Sapienza,'' Unita' di ricerca dell'Istituto Nazionale di Fisica della Materia, piazzale Aldo Moro 2, 00185 Roma, Italy

(Received 22 July 1996)

We report neutron diffraction measurements for two Ne-Xe mixtures at $T=275$ K and $P=26$ MPa, having a Xe molar fraction of 0.81 and 0.45, respectively. These thermodynamic points are chosen to be in the single phase region, close to the gas-gas demixing surface. Total structure factors and neutron weighted pair distribution functions have been extracted. Partial pair distribution functions $g_{ij}(r)$ have been calculated by means of molecular dynamics simulation using Lennard-Jones interaction potentials and the Lorentz-Berthelot mixing rules, obtaining a good agreement with the experimental data. These partial pair distribution functions have been analyzed in terms of density expansion and also compared with those derived in a previous experiment on a He-Xe mixture. The main difference found between the structural properties of the two mixtures is that, in the Ne containing mixture, a definitely larger fraction of atoms of the lighter species occupies the Xe-Xe first neighbor shell. The model already used in interpreting the thermodynamic behavior of the He-Xe mixture in terms of microscopic properties suggests that this structural difference is related to the different behavior of the pressure-temperature projection of the critical line in the two mixtures. [S1063-651X(96)12812-9]

PACS number(s): 61.20.Ja, 61.12.−q, 61.20.Ne

I. INTRODUCTION

In the last decade there has been an increasing effort in understanding the behavior of supercritical fluids [1]. Among these, rare gas mixtures, which exhibit gas-gas demixing phase transitions, are of great interest from a basic research point of view. These phase equilibria are often classified as first or second type according to the behavior of the pressure-temperature projection of the critical line [2]. In the first type equilibria (e.g., He-Xe) the branch of the critical curve which starts from critical point of the less volatile component has always $dP_c/dT_c>0$, while in those of the second type it generally starts with $dP_c/dT_c<0$, and exhibits a temperature minimum before running steeply towards increasing temperatures and pressures (e.g., Ne-Xe).

This is, however, a purely macroscopic classification, while it would be interesting to investigate whether the type of phase equilibrium is related to some microscopic property of the mixture. With this aim we have recently performed a neutron diffraction measurement for the He-Xe mixture near the gas-gas demixing transition at 30 MPa [3]. The analysis of the neutron diffraction data, performed with the help of molecular dynamic (MD) simulations, has shown that (i) the Xe-Xe correlations in the mixture are practically unaffected by the presence of He; (ii) the He-He correlations are strengthened by the presence of Xe, although they are not appreciably modulated by the Xe-Xe correlations; (iii) the He distribution around a given Xe atom is almost homogeneous except for a small excess at a distance of $r\sim 3.3$ Å, i.e., well before the peak of the Xe-Xe first neighbor shell.

These features suggested that the isobaric demixing curves behave *de facto* as the liquid-gas transition of pure Xe, the only difference being a shift of the critical demixing point to higher temperatures and pressures when the He concentration in the mixture is increased. For this reason the difference in the Xe number density between the two coexisting phases seems to be a good order parameter in describing this gas-gas demixing transition. The increase in temperature occurs since the inclusion of He atoms in the Xe first neighboring shell, implied by point (iii), increases the effective two-body interaction between the Xe atoms themselves. The increase of critical pressure with He concentration is mainly a trivial consequence of the difficulty in confining the He atoms inside the mixture. It is therefore interesting to determine the microscopic structure of the Ne-Xe supercritical mixture in which, although the interatomic interactions are not very different from those of the He-Xe mixture, a second type of gas-gas phase equilibrium is known to occur [5].

For these reasons we performed neutron diffraction measurements and MD simulations for two Ne-Xe mixtures (hereafter referred to as mix I and mix II) in thermodynamic states having $P=26.0$ MPa, $T=275.3$ K, and Xe molar fractions $c_{\mathrm{Xe}}=0.81$and $c_{\mathrm{Xe}}=0.45$. These states are very close to the Ne-Xe demixing curve and correspond to those already studied for He-Xe [3].

II. EXPERIMENT

The neutron-diffraction measurements were performed on the 7C-2 diffractometer at the Orphée reactor [6] using neutrons of $\lambda = 1.093$ Å obtained from a Ge(111) monochromator. The samples were contained in a cylindrical cell having an external diameter of 9.5 mm, a wall thickness of 1 mm, and a height of 100 mm, only 50 mm of which were crossed by the neutron beam. The cell was made of vanadium in order to deal with an almost purely incoherent scatterer. It was mounted in a copper holder provided with a thermally controlled flow of cryogenic fluid. The temperature of the cell was measured by means of a thermocouple with an accuracy of ± 0.1 K, and the pressure by means of a strain-gauge detector with an accuracy of better than 0.3 MPa. Temperature gradients across the cell as well as temperature and pressure fluctuations during the runs were within the accuracy of the measurements. With the state parameters chosen the system was always kept slightly above the coexistence curve [5], thus avoiding the risk of having demixing instabilities inside the cell. Gas samples of 99.995% purity were supplied by the Matheson Co. The mixtures were prepared in a reservoir (having a volume V_r of about 50 cm^3) using the following procedure.

(i) The empty reservoir is kept at a fixed temperature ($T = 298$ K) and filled with pure Xe at a given pressure (270 and 71 bar for mix I and mix II, respectively), thus obtaining correspondingly the Xe densities $\rho_{\mathrm{gas}}^{\mathrm{Xe}}$ obtained from Ref. [7].

(ii) The reservoir is then cooled down to 77 K, so that the Xe content solidifies occupying a volume $V = V_r \rho_{\mathrm{gas}}^{\mathrm{Xe}} / \rho_{\mathrm{solid}}^{\mathrm{Xe}}$ where $\rho_{\mathrm{solid}}^{\mathrm{Xe}} = 2.78 \times 10^{-2}$ mole/cm^3 [7] is the density of Xe in the solid phase at $T = 77$ K.

(iii) The empty volume of the reservoir, $(V_r - V)$, is then filled with Ne until the pressure reaches the value (65 and 73 bar for mix I and mix II, respectively) derived [7] for the Ne gas at $T = 77$ K and at the appropriate density, namely, $\rho^{\mathrm{Ne}} = (1/c_{\mathrm{Xe}} - 1)/(1/\rho_{\mathrm{gas}}^{\mathrm{Xe}} - 1/\rho_{\mathrm{solid}}^{\mathrm{Xe}})$, which yields the desired mixture independently on the value of the initial volume V_r.

(iv) The reservoir is finally heated above the demixing temperature. The homogeneity of the mixture is favored stimulating convective motions by the application of thermal gradients opposite to the gravitational field.

The following neutron diffraction measurements have been performed.

(1) Cell filled with sample α, (I_α^E), with $\alpha = 1$ or 2 corresponding to mix I or mix II, respectively.

(2) Empty cell (I_C^E).

(3) Vacuum background (no material in the beam) (I_B^E).

(4) Cadmium rod having the same dimensions of the cell (I_{Cd}^E).

(5) Vanadium rod having the same dimensions of the sample (I_V^E).

For each run the counts of the 640 cells of the positions-sensitive detector (PSD) [8] were recorded in blocks of equal monitor counts (10^6 monitor counts correspond to approximately 1 h). In such a way we have checked that no spurious fluctuations occurred during the run since all the blocks agreed within their statistical errors. At the end of each run the total counts of each PSD cell were normalized to 10^6 monitor counts, obtaining the quantities labeled as I^E.

For each PSD cell (i.e., for each scattering angle) we accumulated approximately 6×10^5 counts for I_α^E ($\alpha = 1,2$), 5.0×10^5 for I_C^E, 6×10^3 for I_{Cd}^E and I_B^E, and 1.2×10^5 for I_V^E. Since I_{Cd}^E and I_B^E are of the order of 3% of I_α^E the statistical error on *each* point of $S(Q)$ can be estimated to be less than 5%. Such an uncertainty is mainly due to the fact that the sample scattering is only about 10% of the total scattering I_α^E.

As far as the Q range is concerned, each measurement extends up to scattering angles of $2\theta = 126°$ and hence up to $Q = 4\pi(\sin\theta)/\lambda \sim 10$ $\mathrm{Å}^{-1}$. The angular resolution is 0.2° and the smallest significant Q value is ~ 0.3 $\mathrm{Å}^{-1}$.

III. DATA ANALYSIS

The differential neutron-scattering cross section per atom in a binary mixture can be written as

$$\frac{\partial \sigma}{\partial \Omega} = (c_1 \overline{b_1} + c_2 \overline{b_2})^2 [S(Q) - 1] + \frac{c_1 \sigma_{s,1}}{4\pi}[1 + P_1(Q)] + \frac{c_2 \sigma_{s,2}}{4\pi}[1 + P_2(Q)], \tag{1}$$

where $\overline{b_j}$ and $\sigma_{s,j}$ are, respectively, the coherent scattering length and the total scattering cross section of species j ($j = 1,2$), c_j its molar fraction, and $P_j(Q)$ the inelasticity correction to the self-scattering contribution. Inelasticity corrections to the interference scattering contribution are assumed, as usual, to be negligible. The total structure factor $S(Q)$, written in terms of the partial structure factors $S_{ij}(Q)$, yields

$$S(Q) - 1 = \frac{1}{(c_1 \overline{b_1} + c_2 \overline{b_2})^2} \{ c_1 \overline{b_1}^2 [S_{11}(Q) - 1] + c_2 \overline{b_2}^2 [S_{22}(Q) - 1] + 2\sqrt{c_1 c_2}\, \overline{b_1 b_2} S_{12}(Q) \}, \tag{2}$$

where the partial structure factors are defined in terms of the pair distribution functions $g_{ij}(r)$ and the partial number densities n_i as

$$S_{ij}(Q) - \delta_{ij} = \sqrt{n_i n_j} \int e^{iQ \times r} [g_{ij}(r) - 1] d^3 r. \tag{3}$$

The neutron weighted pair distribution function $g(r)$ is defined as the Fourier transform of the total structure factor being

$$S(Q) - 1 = n \int e^{iQ \times r} [g(r) - 1] d^3 r, \tag{4}$$

where n is the total number density of the mixture.

In order to derive the total structure factors $S_\alpha(Q)$ from the measured intensities $I_\alpha^E(2\theta)$ we follow the procedure described in [3] [steps from (a) to (d)] for background, empty-cell, multiple-scattering, and absorption corrections. In particular, the single-scattering intensities I_α^S can be expressed in terms of the background-corrected intensity I_α using the relationship

TABLE I. Average values for the parameters employed in the data analysis. Average values are reported since the calculated angular dependence is found to be extremely weak.

	γ_α	m_α	A_α
Mix I	0.952	0.108	0.805
Mix II	0.979	0.105	0.844

$$I_\alpha^S=\frac{1}{A_\alpha}[I_\alpha-\gamma_\alpha I_C-m_\alpha|(I_\alpha-\gamma_\alpha I_C-m_\alpha)/(m_\alpha+1)|_{Q\to\infty}], \tag{5}$$

where γ_α, m_α, and A_α are smooth functions of Q, calculated following Ref. [8]. In these calculations the neutron-beam profile has been assumed to be Gaussian with a full width at half maximum of 1.5 cm as already found in previous measurements which used the same collimators and similar cells [3].

The atomic number densities of the investigated mixtures are needed in order to determine γ_α, m_α, and A_α. Since these are presently not accurately known we have used an iterative procedure based on the internal intensity calibration using the absolute cross section values. The starting density values have been derived from the van der Waals equation using the usual Lorentz-Berthelot combination rule. These density values $n_\alpha^{(0)}$ have been used to calculate the quantities entering Eq. (5), thus deriving zero order single scattering intensities $[I_\alpha^S(Q)]^{(0)}$. These are then used to obtain new density values $n_\alpha^{(1)}$ from the normalization to the vanadium intensity and from the knowledge of the atomic cross sections being

$$\frac{[I_\alpha^S(Q)]_{Q\to\infty}^{(0)}}{I_V^{\rm corr}(Q)A_\alpha^{(0)}}=\frac{n_\alpha^{(1)}\sigma_\alpha}{n_V\sigma_V}, \tag{6}$$

where n_V and σ_V are the atomic number density and the incoherent cross section of vanadium and $I_V^{\rm corr}$ is the intensity scattered by the vanadium sample corrected for multiple scattering, absorption, and inelasticity (see Ref. [9]). Iterating this procedure (typically four times) we obtain values of $(n_\alpha^{(n)}-n_\alpha^{(n+1)})/n_\alpha^{(n)}$ which are less than 0.01. We find $n=0.00785$ Å^{-3} for mix I, and $n=0.00525$ Å^{-3} for mix II. Final values for γ_α, m_α, and A_α are reported in Table I.

Using these values and Eq. (1) the total structure factors are then obtained as

$$S_\alpha(Q)-1=\frac{1}{(c_1^\alpha\overline{b_1}+c_2^\alpha\overline{b_2})^2}\Bigg[L_\alpha^{-1}I_\alpha^S(Q) - \frac{c_1^\alpha\sigma_{s,1}}{4\pi}[1+P_1(Q)] \tag{7}$$

$$- \frac{c_2^\alpha\sigma_{s,2}}{4\pi}[1+P_2(Q)]\Bigg], \tag{8}$$

where

$$L_\alpha(Q)=\frac{A_\alpha n_\alpha I_V^{\rm corr}}{n_V\sigma_V}4\pi \tag{9}$$

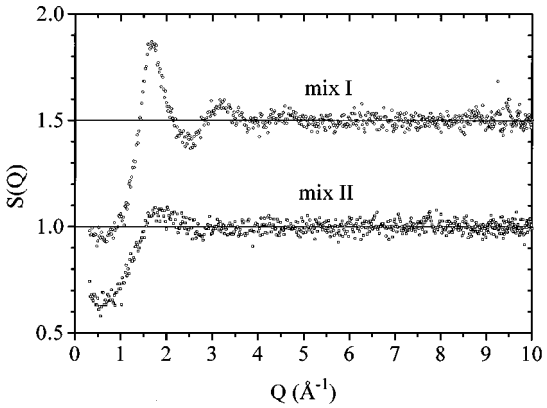

FIG. 1. Experimental structure factors $S(Q)$ for mix I and mix II. The former has been shifted upwards by 0.5.

is the spectrometer luminosity. The inelasticity corrections $P_j(Q)$ have been evaluated using the first-order Placzek expansion, which reads [12]

$$P_j(Q)=\frac{kT}{2E_0m_j}(1-BQ^2), \tag{10}$$

where m_j is the mass of the atom j relative to the neutron mass, E_0 the incident neutron energy, and B is determined by the detector efficiency and by kT/E_0 (see also [6,8]). The values of b and σ_s for V, Ne, and Xe have been taken from [10]. Total structure factors obtained in such a way for the two mixtures are reported in Fig. 1 and are available in ASCII format on request [11].

From the total structure factors, neutron weighted pair distribution functions $g(r)$ are obtained inverting Eq. (4) after introducing the modification function $M(Q)$, described in Ref. [4], in order to reduce spurious oscillations arising from the noise in the high Q data; in the present case we have used $Q_i=4$ Å and $Q_f=7$ Å. As an example we show in Fig. 2 the $g(r)$ obtained for mix I.

Exploiting the physical constraint that $g(r)$ must vanish for distances less than the minimum approach distance, we can further account for minor inadequacies in the corrections calculated above subtracting a low-order polynomial from

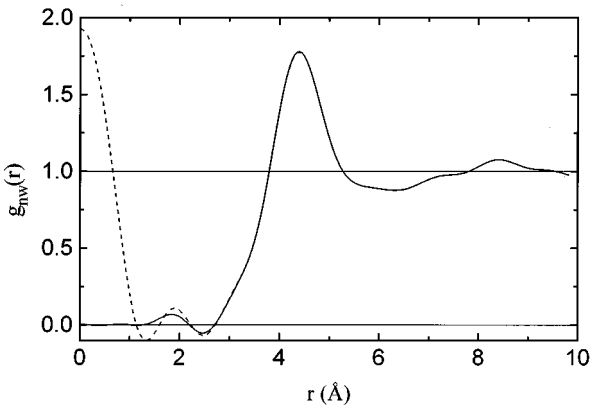

FIG. 2. Experimental neutron weighted pair distribution function $g(r)$ for mix I (dashed line) together with the refined $g^{\rm corr}(r)$ (solid line).

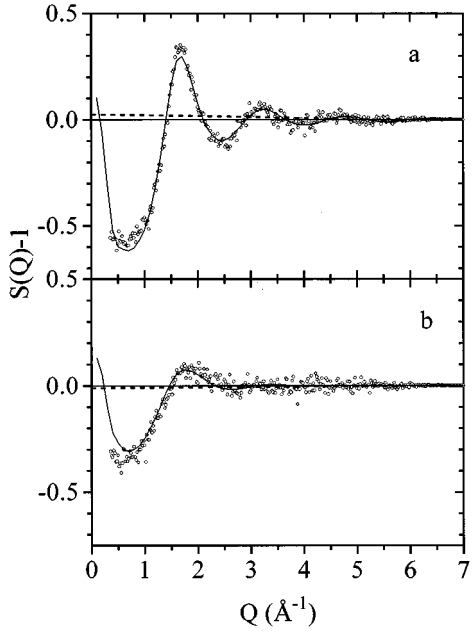

FIG. 3. Total structure factors for (a) mix I; (b) mix II. Refined $S^{\mathrm{corr}}(Q)$ (open circles), polynomial correction (dashed line), MD simulation (solid line).

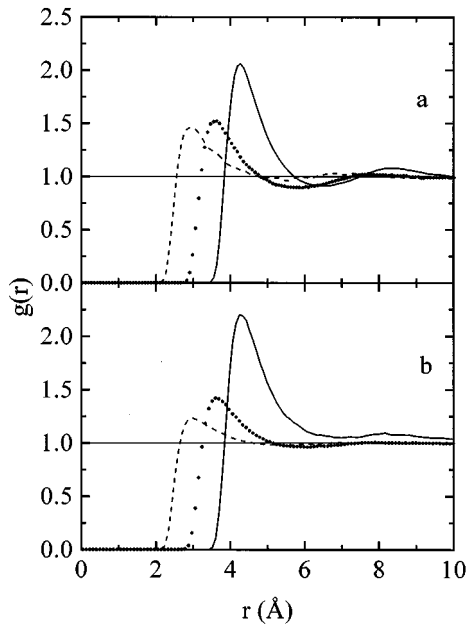

FIG. 4. MD partial pair distribution functions for (a) mix I; (b) mix II. $g_{\mathrm{XeXe}}(r)$ (solid line), $g_{\mathrm{NeXe}}(r)$ (dotted line), $g_{\mathrm{NeNe}}(r)$ (dashed line).

the data. The coefficients of the polynomial have been determined using a least square procedure which minimizes the resulting $g(r)$ up to the minimum approach distance. The resulting $g(r)$, quoted as $g^{\mathrm{corr}}(r)$, is also reported for mix I in Fig. 2; the improved structure factor, $S^{\mathrm{corr}}(Q)$, as well as the polynomial found for both mixtures, are shown in Figs. 3(a) and 3(b).

For a deeper understanding of the neutron diffraction results we have also performed a molecular dynamics simulation in order to evaluate the partial pair distribution functions $g_{ij}(r)$. The following Lennard-Jones parameters have been used:

$$\epsilon_{\mathrm{XeXe}}/k = 230\ \mathrm{K}; \quad \sigma_{\mathrm{XeXe}} = 3.85\ \mathrm{A}, \quad \epsilon_{\mathrm{NeNe}}/k = 35.1\ \mathrm{K};$$

$$\sigma_{\mathrm{NeNe}} = 2.72\ \mathrm{A}, \quad \epsilon_{\mathrm{NeXe}}/k = (\epsilon_{\mathrm{NeNe}}\epsilon_{\mathrm{XeXe}})^{0.5};$$

$$\sigma_{\mathrm{NeXe}} = (\sigma_{\mathrm{NeNe}} + \sigma_{\mathrm{XeXe}})/2. \tag{11}$$

The reliability of the pair potential used in the present simulation for the pure species has been successfully tested in a previous paper by comparing the numerical results with those of a neutron diffraction experiment [4].

For both mixtures a time step of 5 fs and a total number of 500 particles has been used. Pair distribution functions $g_{ij}(r)$ are calculated as an average over 10^5 time steps after thermalizing the samples for about 7×10^4 time steps; they are reported in Figs. 4(a) and 4(b). From the $g_{ij}(r)$ we have evaluated $S(Q)$ and $S_{ij}(Q)$ through Eqs. (2) and (3). The $S(Q)$ so obtained are also reported in Fig. 3. For comparison we also evaluated analytically the first-order density expansion of $g_{ij}(r)$ as already done in Eqs. (8)–(10) of Ref. [3]; they are shown in Figs. 5 and 6 for Xe-Xe and Ne-Ne, respectively.

IV. DISCUSSION

The agreement between the experimental and the simulated $S(Q)$, as shown in Fig. 3, is very good for both mixtures. As in the case of the He-Xe mixture, this fact suggests that the MD simulations, with the intermolecular potential defined in the preceding section, well reproduce the micro-

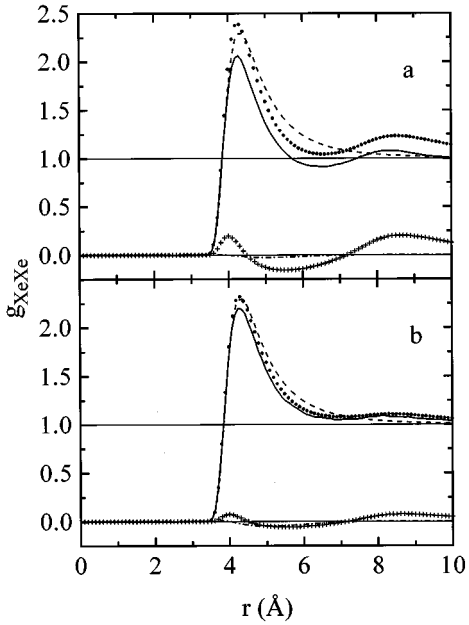

FIG. 5. $g_{\mathrm{XeXe}}(r)$ obtained using Lennard-Jones potentials for (a) mix I; (b) mix II . Zeroth-order contribution $g^{(0)}(r)$ (dashed line); first-order correction due to the surrounding Xe atoms (crosses); first-order correction due to the surrounding Ne atoms (dash-dotted line); full density expansion up to the first-order $g^{(1)}_{\mathrm{XeXe}}(r)$ (dotted line); MD results (solid line).

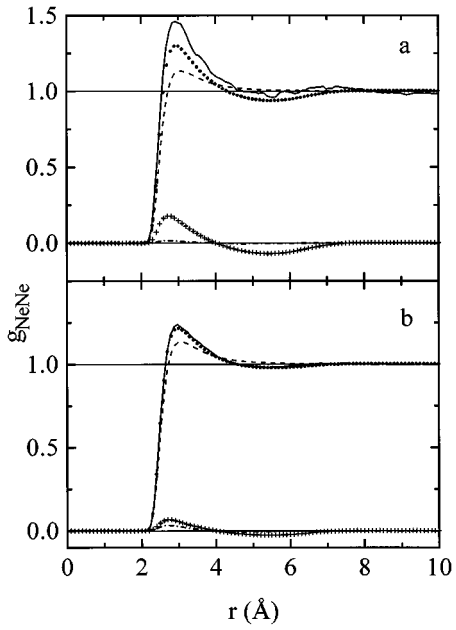

FIG. 6. $g_{\mathrm{NeNe}}(r)$ obtained using LJ potentials for (a) mix I; (b) mix II. Zeroth-order contribution $g^{(0)}(r)$ (dashed line); first-order correction due to the surrounding Xe atoms (crosses); first-order correction due to the surrounding Ne atoms (dash-dotted line); full density expansion up to the first-order $g^{(1)}_{\mathrm{NeNe}}(r)$ (dotted line); MD results (solid line).

scopic structure of the real system. In particular we can conclude that the three partial pair distribution functions $g_{\mathrm{NeNe}}(r)$, $g_{\mathrm{NeXe}}(r)$, $g_{\mathrm{XeXe}}(r)$ obtained from MD can be safely used to discuss also the structure of the real Ne-Xe mixture. We will discuss first the results relative to mix I.

A. Xe-Xe correlations

The Xe-Xe correlations in the mixture appear to be very weakly affected by the presence of Ne atoms. The reduced influence of Ne atoms on the Xe-Xe correlations in the mixture can be better understood by comparing the $g_{\mathrm{XeXe}}(r)$ function in the mixture and the one obtained by MD simulation of pure Xe having the same Xe number density as mix I; the two are found to coincide well within 1%. This is consistent with the fact that the contribution of the Ne atoms to the first-order term in $g_{\mathrm{XeXe}}(r)$ density expansion is practically negligible [see Fig. 5(a)].

The same conclusion, concerning the influence of the lighter species on the Xe-Xe structure, was reached for the He-Xe mixture [3]. Moreover, the Xe-Xe distribution functions yield in both cases a value of about 5.6 atoms in the first neighbor shell (i.e., up to the 5.7 Å).

B. Ne-Ne correlations

The structural implications of the MD results for these correlations can be understood by looking at Fig. 6(a) where the density expansion of $g_{\mathrm{NeNe}}(r)$ is reported. It appears that the position of the first peak is mainly determined by the Ne-Ne interaction [it has indeed the same position as in $g^{(0)}_{\mathrm{NeNe}}(r)$] while the Xe-Ne interactions act only to increase the peak intensity and to produce a clear minimum giving a better definition of the first neighbor shell. Moreover, among the first-order terms of the density expansion, those involving only Ne-Ne interactions give a practically negligible contribution to $g_{\mathrm{NeNe}}(r)$.

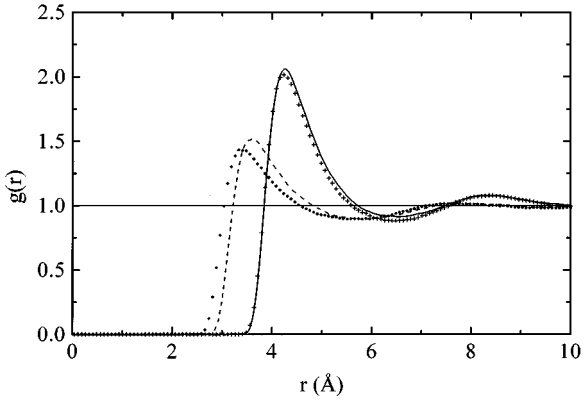

FIG. 7. MD partial distribution functions: $g_{\mathrm{XeXe}}(r)$ for mix I from present experiment (solid line) and for mix I from Ref. [3] (crosses); $g_{\mathrm{NeXe}}(r)$ for mix I from present experiment (dashed line), and $g_{\mathrm{HeXe}}(r)$ for mix I from Ref. [3] (dotted line).

C. Ne-Xe correlations

These correlations show a well defined peak at $r=3.6$ Å [see Fig. 4(a)]. Since this value is rather close to the Xe-Xe minimum approach distance there is a significant overlap between the Ne-Xe and Xe-Xe first neighbor shells. A deeper understanding can be achieved by comparing the present results with those of the previous experiment performed with He-Xe mixture at similar temperature and density [3]; this comparison is shown in Fig. 7 from which we derive that the number of first neighbor atoms of the lighter species around the Xe atoms is in both cases about 0.7. However if we calculate the fraction of first Ne (or He) neighbors around a Xe atom which are not overlapping with the first neighbor Xe atoms (i.e., for $r<3.5$ Å) we obtain 0.33 in the case of the Ne-Xe mixture and 0.47 in the He-Xe one. Following the conclusions of Ref. [3], reported also in the Introduction of the present paper, this increased overlap influences the Xe-Xe two-body effective interaction and therefore the critical demixing temperature.

As far as mix II is concerned, the conclusions about the partial distribution functions are substantially the same as in the case of mix I except that in the present case the behavior of the various partial $g_{ij}(r)$ functions is more gaslike. The density expansion up to first order is indeed sufficient to reproduce the MD results; these points are clearly shown in Figs. 5(b) and 6(b).

V. CONCLUSIONS

Our neutron diffraction measurements, together with MD simulations, exhibit the following relevant features.

(1) The Xe-Xe correlations in the mixture are only very weakly affected by the presence of Ne atoms.

(2) The Ne-Ne correlations are strengthened by the presence of Xe but they are not appreciably modulated by the Xe-Xe correlations.

(3) Compared to what happens in the He-Xe mixture, a

definitely larger fraction of atoms of the lighter species occupy the Xe-Xe first neighbor shell.

These conclusions, compared with those obtained for the He-Xe mixture, imply that the different kind of supercritical demixing transitions exhibited by the two mixtures (as determined by the sign of dP_c/dT_c) could be related to differences in the unlike atomic pair distributions.

However, we want to stress that these considerations should be taken as rather qualitative guesses which require further and more quantitative investigations. A theoretical approach in this direction based on the van der Waals equation of state is in progress.

[1] J. M. H. Levelt Sengers, in *Supercritical Fluids*, Vol. 273 of *NATO Advanced Studies Institue, Series E , Applied Science*, edited by E. Kiran and J. M. H. Levelt Sengers (Kluwer, Dordrecht, 1994).

[2] G. M. Schneider, Adv. Chem. Phys. **17**, 1 (1970).

[3] M. C. Bellissent-Funel, U. Buontempo, A. Filabozzi, M. Nardone, and F. P. Ricci, Phys. Rev. A **46**, 1002 (1992).

[4] M. C. Bellissent-Funel, U. Buontempo, A. Filabozzi, C. Petrillo, and F. P. Ricci, Phys. Rev. B **45**, 4605 (1992).

[5] A. Deerenberg, J. A. Schouten, and N. J. Trappeniers, Physica A **101**, 459 (1980).

[6] J. P. Ambroise, M. C. Bellissent-Funel, and P. R. Bellissent, Rev. Phys. Appl. **19**, 731 (1984).

[7] A. Michels, T. Wassenaar, and P. Louwerse, Physica **20**, 99 (1954); J. A. Beattie, in *Argon, Helium and the Rare Gases*, edited by G.A. Cook (Interscience Publishers, New York, 1961), Vol. 1.

[8] J. P. Ambroise and P. R. Bellissent, in *Position Sensitive Detection of Thermal Neutrons*, edited by P. Convert and J. B. Forsyth (Academic, New York, 1983), p. 286.

[9] C. Petrillo and F. Sacchetti, Acta Crystallogr. Sect. A **46**, 440 (1990).

[10] S. W. Lovesey, in *Theory of Neutron Scattering from Condensed Matter*, 2nd ed. (Oxford University Press, Oxford, 1986), Vol. 1.

[11] Total structure factors are available as ASCII files from M. Nardone. Electronic address: nardone@axcasp.caspur.it

[12] R. Winter and T. Bodensteiner, in *High Pressure Research* (Gordon and Breach, New York, 1988), Vol. 1, p. 23.